






Original Research

Fto-Mediated m6A Demethylation of *Anxa1* Attenuates Cardiac Ischemia–Reperfusion Injury With Suppression of Nlrp3 Inflammasome Signals

Chaojie He^{1,†} , Haojie Yang^{1,†} , Lijia Xu¹ , Hao Zhang² , Huilin Hu^{1,*} 
¹Department of Cardiology, The Affiliated Hospital of Jiaxing University, 314000 Jiaxing, Zhejiang, China

²Rhine-nahr-palatinate Heart and Vascular Center, 55543 Bad Kreuznach, Germany

*Correspondence: huhuulin1979@sohu.com (Huilin Hu)

†These authors contributed equally.

Academic Editor: Natascia Tiso

Submitted: 30 May 2025 Revised: 1 September 2025 Accepted: 5 September 2025 Published: 28 September 2025

Abstract

Background: Myocardial ischemia-reperfusion (I/R) injury represents the major obstacle to achieving successful therapeutic outcomes in acute myocardial infarction patients. Fat mass and obesity-associated protein (Fto), an N6-methyladenosine (m6A) RNA demethylase, has been shown to protect cardiomyocytes against oxygen-glucose deprivation/reperfusion-mediated injury by regulating annexin A1 (*Anxa1*) expression *in vitro*. The present study aims to confirm the cardioprotective role of the Fto/*Anxa1* axis using *in vivo* myocardial I/R injury models. **Methods:** Wild-type (WT) and *Anxa1* knockout (KO) mice underwent 30-min left coronary artery ligation and 2-h reperfusion after intramyocardial delivery of recombinant adeno-associated virus serotype 9 encoding *Fto* (*adFto*) or a control vector (*adnull*). The effects of Fto overexpression on cardiac function, fibrosis, apoptosis, and inflammatory response were examined using echocardiography, Masson's trichrome staining, western blot analysis, enzyme-linked immunosorbent assay, and immunohistochemical staining. m6A-RNA immunoprecipitation-quantitative polymerase chain reaction quantified *Anxa1* mRNA methylation. **Results:** Fto overexpression by *adFto* significantly improved cardiac function, reduced serum creatine kinase-myocardial band and troponin T levels, and alleviated cardiac fibrosis in I/R-injured WT mice. Mechanistically, Fto weakened I/R-induced global m6A levels and decreased m6A enrichment on *Anxa1* mRNA, thereby enhancing *Anxa1* expression. In *Anxa1* KO mice, *adFto* did not confer functional or molecular benefit. **Conclusions:** Fto enhances *Anxa1* and mitigates myocardial I/R injury with suppression of nucleotide-binding oligomerization domain-, leucine-rich repeat-, and pyrin domain- containing receptor 3 (*Nlrp3*)-inflammasome signaling *in vivo*, identifying the Fto-*Anxa1* axis as a mechanistic contributor and potential therapeutic target.

Keywords: myocardial reperfusion injury; annexin A1; RNA methylation; demethylation; inflammasomes

1. Introduction

Acute myocardial infarction (MI), resulting from acute coronary artery occlusion, represents a leading cause of mortality among cardiovascular disease patients [1]. Although timely reperfusion remains the most effective clinical strategy for myocardial salvage, revascularization paradoxically triggers myocardial ischemia-reperfusion (I/R) injury, contributing to approximately 50% of the final infarct size [2]. Current therapeutic strategies for myocardial I/R injury primarily encompass non-pharmacological interventions, pharmacological therapies, and administration of human-induced pluripotent stem cells, yet clinical trials have demonstrated suboptimal outcomes [3,4]. Consequently, elucidating the molecular pathways governing myocardial I/R injury progression and identifying novel therapeutic targets for effective clinical interventions are imperative.

Dynamic RNA epigenetic modifications, especially the reversible N6-methyladenosine (m6A) methylation, are increasingly recognized as pivotal regulators in cardiovascular pathophysiology [5]. m6A is installed by the

Methyltransferase-like (Mettl13-Mettl14) complex and removed by the demethylase Fat mass and obesity-associated protein (Fto), enabling rapid remodeling of mRNA fate in response to stress [6,7]. During acute stress, m6A landscapes are reprogrammed to control the translation and stability of selective transcripts, thereby modulating adaptive responses [8]. In the heart, abrupt I/R and chronic comorbidities such as diabetes and hypertension represent prototypical stress contexts in which such post-transcriptional control becomes crucial. As a critical m6A demethylase, Fto is implicated in the pathogenesis of various cardiovascular disorders [9]. Yang *et al.* [10] revealed that Fto alleviates doxorubicin-induced cardiotoxicity by activating the cyclin-dependent kinase inhibitor 1A (P21)/nuclear factor erythroid 2-related factor 2 (*Nrf2*) pathway via m6A demethylation of tumor protein p53 or P21/*Nrf2*. Moreover, Fto mitigates myocardial I/R injury by inhibiting nucleotide-binding oligomerization domain-, leucine-rich repeat-, and pyrin domain- containing receptor 3 (*Nlrp3*)-mediated pyroptosis via regulating casitas B lineage lymphoma mRNA stability and its dependent β -catenin ubiqu-



uitination/degradation [11]. The importance of mitochondrial homeostasis in myocardial I/R is well supported by experimental evidence, highlighting it as a targetable node in cardio-protection [12]. Consistently, Fto protects the myocardium via m6A-dependent stabilization of peroxisome proliferator-activated receptor gamma coactivator 1 alpha mRNA, leading to enhanced mitochondrial biogenesis and reduced oxidative stress [13]. Although Fto has been established to engage in myocardial I/R injury, the mechanism by which it mediates has not been fully elucidated.

As an endogenous anti-inflammatory molecule, *Annxin A1* (*Anxa1*) plays a pivotal role in modulating inflammatory responses and cell survival [14]. Available evidence suggested that *Anxa1* is closely associated with myocardial I/R injury. Recombinant *Anxa1* reduces infarct size by 50% [15], and administration of *Anxa1*-derived peptide Ac2-26 shrinks infarct size and reduces myeloperoxidase and interleukin (IL)-1 β levels in infarcted hearts [16]. Qin *et al.* [17] disclosed that endogenous administration of Ac2-26 boosts cardiomyocyte viability and recuperates left ventricular function at the onset of reperfusion. However, a clinical trial uncovered that elevated *Anxa1* levels are associated with severe congestion, worsened renal function, severe disease, and worse prognosis in patients with acute heart failure and impaired renal function [18]. Our findings demonstrated that Fto-mediated demethylation of *Anxa1* attenuates *Nlrp3*-mediated pyroptosis and inflammation, thereby protecting cardiomyocytes from I/R injury at the cell level *in vitro* [19], yet the cardioprotective effects of the Fto/*Anxa1*/*Nlrp3* axis in a complex living environment still need to be validated by animal experiments.

The study focused on verifying the epigenetic regulatory mechanism of the Fto/*Anxa1*/*Nlrp3* axis in myocardial I/R injury in animal models, thereby providing potential therapeutic targets for novel interventions.

2. Materials and Methods

2.1 Animals

All experimental procedures involving animals were undertaken in accordance with the National Institutes of Health guidelines and received approval from the Animal Care and Use Committee of Jiaying University Medical College (Approval No. JUMC2021-095). Wild type (WT) C57BL/6 mice (6–8 weeks old; Cyagen, Suzhou, Jiangsu, China) and *Anxa1* knockout (KO) mice with a C57BL/6 background (6–8 weeks old; Cyagen, Suzhou, Jiangsu, China) were maintained in a specific pathogen-free facility under controlled conditions: relative humidity 40–70%, ambient temperature of 20–25 °C, 12-h light/dark cycle, and free access to food/water. Euthanasia was induced by placing animals in a chamber pre-filled with 100% medical-grade CO₂ at a flow rate displacing 30–70% of the chamber volume per minute. After ≥ 5 min post-respiratory arrest, cervical dislocation was performed at the C1–C2 vertebrae to confirm death. To eliminate potential confounding

effects of female sex hormones, only male mice were utilized. To minimize bias, a randomized allocation protocol was implemented. Mice were randomly assigned to either experimental or control cohorts. Cardiac I/R injury modeling and echocardiographic assessments were conducted by an operator blinded to group assignments. Group allocation information was concealed from the operator throughout both the experimental execution and subsequent data analysis phases, ensuring blinding integrity.

2.2 Mouse MI Model

Following standard procedures, mice underwent a transient left anterior descending (LAD) coronary artery occlusion to induce cardiac I/R injury. Under general anesthesia (2% isoflurane), mice underwent endotracheal intubation with mechanical ventilation support. A 5-mm left thoracotomy between the 4th and 5th intercostal spaces was performed to expose the cardiac apex. A silk suture (8-0) was positioned 2–3 mm distal to the LAD origin, adjacent to the junction of the left atrial appendage and pulmonary artery. Coronary occlusion was achieved by tightening the suture loop, with successful ischemia induction confirmed by ST-segment elevation on continuous electrocardiogram monitoring and pallor of the distal myocardium. Following 30 min of ischemia, reperfusion (2 h) was initiated by suture release, evidenced by myocardial blush restoration. Postoperatively, mice were allowed to recover from anesthesia on a warm pad with *ad libitum* access to water and moistened chow. Sham-operated mice underwent identical procedures except for coronary occlusion (no LAD ligation).

2.3 Animal Grouping

WT mice were randomized into 3 groups in part I (sham, MI + adnull, and MI + adFto; n = 6). WT and *Anxa1* KO mice were respectively randomized into 3 groups in part II (sham, MI + adnull, and MI + adFto; n = 6). Fto overexpression was achieved in MI mice via intramyocardial injection of a recombinant adeno-associated virus serotype 9 vector (AAV9) encoding Fto (adFto). Both adFto and a control vector (adnull) were purchased from Genechem (Shanghai, China). To ensure sufficient protein overexpression during cardiac I/R injury, intramyocardial delivery of ad vectors (adFto/adnull, 1×10^9 vg/mouse) was performed via left ventricular multi-point injection. Using a 30-gauge ultrafine needle coupled to an insulin syringe, a total of 20 μ L AAV9 was delivered as four 5 μ L intramyocardial injections into the left-ventricular anterior wall bordering the ischemic area, from apex to base, using a 30-gauge Hamilton syringe, with approximately 60 s per site [20].

2.4 Transthoracic Echocardiography (Echo)

Cardiac functional evaluation was performed using a transthoracic echocardiography (RMV-707B; VisualSonics, Toronto, ON, Canada) with a Vevo 2100 high-resolution imaging system (FujiFilm VisualSonics, Inc.,

Toronto, ON, Canada) equipped with a 40-MHz single-element transducer. Following anesthesia induction via 2% isoflurane, mice were maintained under 0.8–1.5% vaporized isoflurane through a gas anesthesia system. M-mode acquisitions were obtained from parasternal long-axis views at papillary muscle level, with 3 consecutive cardiac cycles recorded for offline analysis. Left ventricular functional indices, including ejection fraction (EF) and fractional shortening (FS).

2.5 Serum Biochemical Analysis

Serum samples were obtained through retro-orbital venous plexus puncture under isoflurane anesthesia (2%–3% for induction and 1%–2% for maintenance). Whole blood was processed by centrifugation (3000 ×g, 15 min, 4 °C) to isolate serum supernatant. Cardiac injury biomarkers, including Troponin T (TnT) and creatine kinase-myocardial band isoenzyme (CK-MB) were quantified using species-specific ELISA kits (#MBS761403/#MBS2701855; MyBiosource, San Diego, CA, USA) following standardized protocols.

2.6 Reverse Transcriptase-Quantitative Polymerase Chain Reaction (RT-qPCR)

Total RNA isolation from heart tissues was conducted with TRIeasy™ total RNA extraction reagent (#10606ES60; Yeasen, Shanghai, China) following standard protocols. First-strand complementary DNA (cDNA) synthesis was subsequently performed using Hifair® II 1st strand cDNA synthesis kit (#11119ES60; Yeasen, Shanghai, China). Quantitative PCR amplification was achieved with Hieff® qPCR SYBR green master mix (high Rox plus; #11203ES08; Yeasen). Gene expression was quantified using the $2^{-\Delta\Delta CT}$ method, normalized to glyceraldehyde-3-phosphate dehydrogenase (Gapdh) expression [21]. Amplification by quantitative PCR employed the subsequent primer sets: *Gapdh*, Forward-5'-CATCACTGCCACCCAGAAGACTG-3', Reverse-5'-ATGCCAGTGAGCTTCCCGTTTCAG-3'; *Anxa1*, Forward-5'-TGTATCCTCGGATGTTGCTGCC-3', Reverse-5'-CCATTCTCCTGTAAGTACGCGG-3'.

2.7 Western Blot

Cardiac tissue homogenization was performed in radioimmune precipitation assay buffer (#G2002; Servicebio, Wuhan, Hubei, China) supplemented with phenylmethane-sulfonyl fluoride (1 mM; #G2008; Servicebio, Wuhan, Hubei, China). Prior to electrophoresis, the protein concentration in each sample was measured with a commercial bicinchoninic acid assay kit (#G2026; Servicebio, Wuhan, Hubei, China). Equal amounts of lysates were resolved through 10–12% sodium dodecyl sulfate–polyacrylamide gel electrophoresis and electrophoretically transferred onto polyvinylidene fluoride membranes, followed by blocking with 5% skim milk/Tris-buffered saline with 0.1% Tween-

20. The membranes were immuno-detected with primary antibodies against Fto, Anxa1, B cell lymphoma-2 (Bcl-2), Bcl-2-associated X protein (Bax), apoptosis-associated speck-like protein (ASC), cleaved-Caspase 1 (cle-Caspase 1), pro-Caspase 1, Nlrp3, gasdermin D-N-terminal domain (N-Gsdmd), gasdermin D (Gsdmd), and Gapdh. Information on all antibodies is displayed in **Supplementary Table 1**. After TBST washing, the membranes were probed with a secondary antibody at ambient temperature for 60 min. Protein signals were developed using an enhanced ECL chemiluminescent substrate kit (#36222ES76; Yeasen). Immunoreactive bands were quantified densitometrically using ImageJ software (1.54p; NIH, Bethesda, MD, USA), with Gapdh serving as the loading control.

2.8 Enzyme-Linked Immunosorbent Assay (ELISA)

The cardiac tissues were cut into small pieces, homogenized, and centrifuged to get the supernatants (5 min, 5000 ×g). The harvested supernatants were employed for the detection of pro-inflammatory cytokines tumor necrosis factor alpha (TNF- α), IL-6, and IL-1 β . All detection steps were performed in strict accordance with the instructions provided with the ELISA kit (#MBS2124239/#MBS450807/#MBS2021142; MyBiosource, San Diego, CA, USA).

2.9 Masson's Trichrome Staining

Cardiac tissues were harvested and fixed in 4% paraformaldehyde (#E672002; Sangon, Shanghai, China), followed by embedding into paraffin and sectioning at 4 μ m intervals. Subsequently, the sections underwent deparaffinization, dehydration via xylene, and ethanol gradient immersion, followed by Masson's trichrome staining according to standard procedures. Collagen fiber content was analyzed according to the following equation: Collagen fiber (%) = (blue area pixels/total area pixels) × 100%.

2.10 Total m6A Detection

Total RNA samples prepared with TRIzol extraction reagent were subjected to m6A quantification via the m6A RNA methylation quantification kit (#P-9005; Epigentek, Flushing, NY, USA). RNA aliquots (200 ng/sample) were sequentially incubated with capture antibody, detection antibody, enhancer solution, and chromogenic substrate in 96-well plates. Absorbance values at 450 nm were measured with a microplate reader (Bio-Rad, Hercules, CA, USA), where experimental values were derived from established standard curve calculations.

2.11 m6A-RNA Immunoprecipitation (RIP)-Quantitative Polymerase Chain Reaction (qPCR)

Total RNA from left ventricles was extracted with TRIzol and treated with DNase I. m6A RNA immunoprecipitation (IP) was performed using an anti-m6A antibody with species-matched IgG as a negative control according to

the manufacturer's protocol. Information on all antibodies is displayed in **Supplementary Table 1**. After IP, RNA was purified, reverse-transcribed, and qPCR was carried out for *Anx1*. Enrichment was quantified as % input and as fold over IgG.

2.12 Immunohistochemistry (IHC) Staining

Paraffin-embedded cardiac tissues were sectioned into 4 μ m sections for IHC analysis with a 3,3-diaminobenzidine (DAB) detection system. Endogenous peroxidase was inactivated by sequential deparaffinization, rehydration, and 15-min incubation in 3% H₂O₂-methanol solution, followed by 20-min antigen retrieval at 95 °C. Tissue sections were treated overnight at 4 °C with anti-Nlrp3 primary antibody (#D261589; at 1:25 dilution; Sangon, Shanghai, China), followed by 30-min incubation with a secondary antibody (#D110073; at 1:1000 dilution; Sangon, Shanghai, China). Reaction products were visualized after counterstaining with the ultra-sensitive horseradish the catalase DAB color kit (#C510023; Sangon, Shanghai, China). Images were captured at 100 \times magnification using a microscope (Olympus, Tokyo, Japan).

2.13 Statistical Analysis

Experimental results are presented as mean \pm standard error of mean (SEM) (minimum 3 repeats). Analyses were conducted in GraphPad Prism 9 (GraphPad Software, San Diego, CA, USA), with multi-group comparisons meeting normality and homogeneity of variance assumptions analyzed by one-/two-way analysis of variance (ANOVA) and Tukey's multiple comparisons test. Statistical significance was defined at $p < 0.05$.

3. Results

3.1 Fto Overexpression Attenuates Cardiac I/R Injury and Elevates *Anx1* Expression in Mouse Models

To verify that Fto-mediated m6A demethylation of *Anx1* mitigates cardiac I/R injury *in vivo*, we injected adFto or adnull intramyocardially in mice, followed by performing the MI surgery and reperfusion (Fig. 1A). Changes in Fto protein levels were detected in heart samples. As expected, MI mouse-derived heart samples possessed lower Fto protein levels than those from sham mice, and administration of adFto increased Fto protein levels in heart samples from MI mice (Fig. 1B). Cardiac function was assessed by Echo, as displayed in Fig. 1C. We observed significant reductions in both EF (56.17% vs. 34.00%, $p < 0.001$) and FS (35.67% vs. 12.67%, $p < 0.001$) values in the hearts of mice subjected to MI, but Fto overexpression improved these reductions (EF: 34.00% vs. 46.67%, $p < 0.001$; FS: 12.67% vs. 20.67%, $p < 0.001$) (Fig. 1D,E). The myocardial injury parameters CK-MB and TnT in the serum of MI mice were significantly higher than those of sham mice (CK-MB: 149.7 mg/mL vs. 902.5 mg/mL, $p < 0.001$; TnT: 2.34 pg/mL vs. 15.02 pg/mL, $p < 0.001$),

yet ectopic expression of Fto ameliorated serum CK-MB (902.5 mg/mL vs. 606.6 mg/mL, $p < 0.001$) and TnT (15.02 pg/mL vs. 12.63 pg/mL, $p < 0.001$) levels for MI mice (Fig. 1F,G). Masson's staining showed a higher content of collagen fibers in MI mouse-derived heart tissues (19.43% vs. 38.80%, $p < 0.001$), but exogenous overexpression of Fto decreased collagen fiber content in heart tissues (38.80% vs. 25.84%, $p < 0.001$) (Fig. 1H,I). Considering that the main role of Fto is demethylation modification, we tested m6A levels in heart tissues. Total m6A levels were significantly up-regulated in heart tissues of MI mice (0.02818% vs. 0.04672%, $p < 0.001$), while exogenous expression of Fto reversed the increase in m6A levels in heart tissues (0.04672% vs. 0.03084%, $p < 0.001$) (Fig. 1J). Moreover, m6A-RIP-qPCR showed that m6A enrichment on *Anx1* decreased with Fto overexpression ($p < 0.001$) (Fig. 1K). IgG controls remained low across groups. These data support Fto-dependent transcript-level demethylation of *Anx1* *in vivo*. Additionally, a significant reduction in mRNA and protein levels of *Anx1* was observed in heart tissues of mice undergoing MI ($p < 0.001$ and $p < 0.001$), whereas exogenous expression of Fto potentially raised *Anx1* mRNA and protein levels ($p < 0.001$) (Fig. 1L,M). Collectively, these results indicate that Fto improved cardiac function and reduced injury and fibrosis in MI hearts, accompanied by reduced m6A enrichment on *Anx1* and increased *Anx1* expression.

3.2 *Anx1* Mediates the Protective Effect of Fto on Cardiac I/R Injury in Mouse Models

To identify that Fto exerts cardioprotective effects by up-regulating *Anx1*, we constructed MI models after adFto or adnull administration using WT or *Anx1* KO mice, followed by reperfusion. Briefly, a 2 \times 2 factorial analysis within MI cohorts (genotype: WT vs *Anx1* KO; treatment: adnull vs. adFto) using two-way ANOVA with a genotype \times treatment interaction. Sham values are provided to illustrate baseline ranges and confirm I/R effects. At the experimental endpoint, *Anx1* protein could not be detected in *Anx1* KO mouse-derived cardiac tissues, and there were no significant differential alterations in Fto protein levels between heart tissues from WT and *Anx1* KO mice (Fig. 2A). We discovered that *Anx1* knockout didn't affect EF values significantly in normal mice, but decreased FS values slightly. Like WT mice, *Anx1* KO mice subjected to MI showed a significant reduction in EF (61.50% vs. 25.17%, $p < 0.001$) and FS (29.67% vs. 15.17%, $p < 0.001$) values. Interestingly, Fto overexpression ameliorated the reduced EF and FS values in WT mice undergoing MI but did not work in *Anx1* KO mice (EF: 25.17% vs. 24.83%, $p > 0.9999$; 15.17% vs. 15.00%, $p > 0.9999$) (Fig. 2B–D). The genotype \times treatment interaction was significant for EF (F [2, 30] = 25.41, $p < 0.001$) and FS (F [2, 30] = 38.14, $p = 0.0130$), indicating that the functional benefit of adFto depends on *Anx1*. Furthermore, adFto reduced CK-

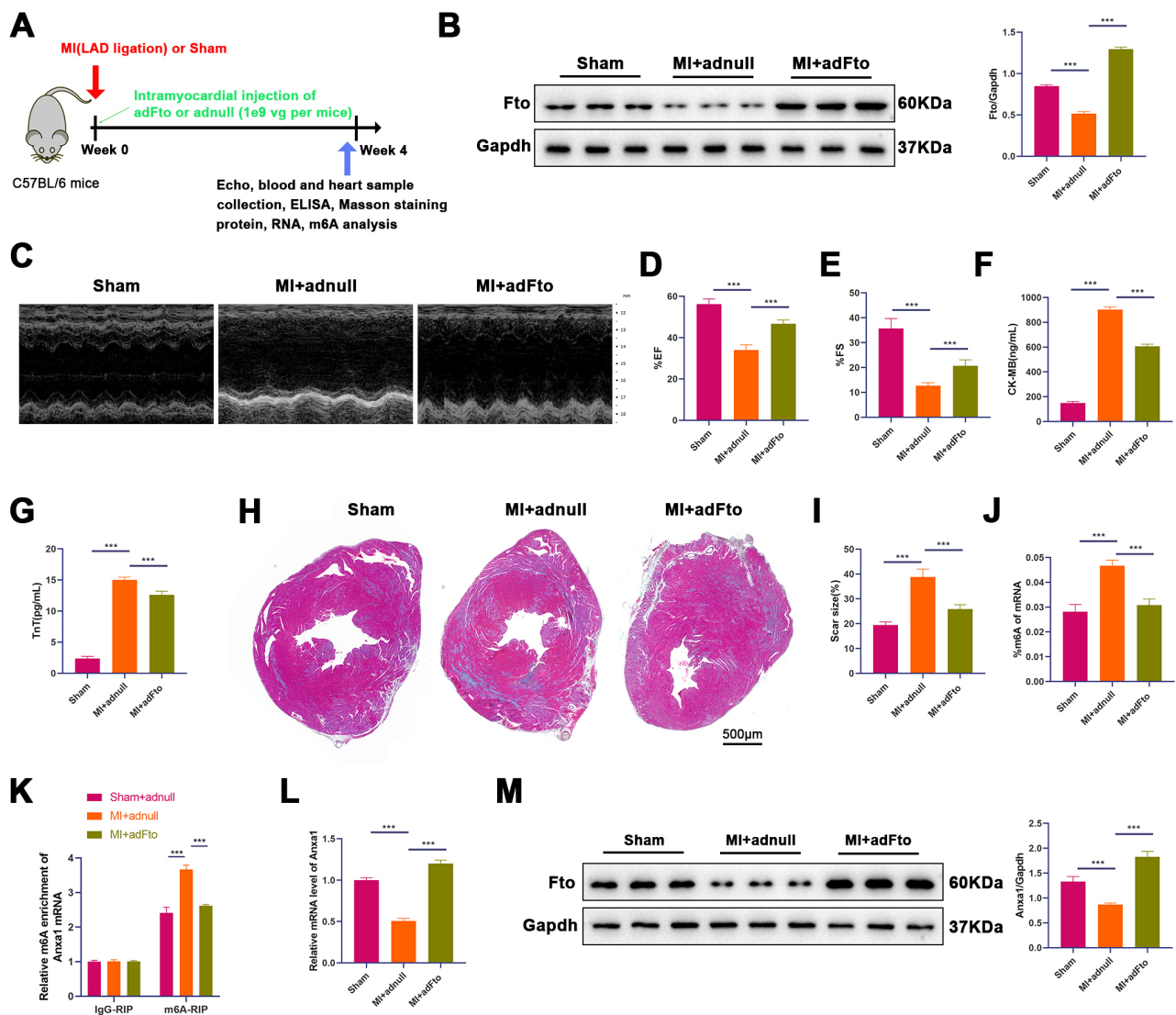


Fig. 1. Fto overexpression alleviates cardiac I/R injury and enhances *Anxa1* expression in mouse models. (A) Experimental strategy in mouse models with MI. Mice underwent LAD occlusion for 30 min after intramyocardial injection of adFto or adnull (1×10^9 vg/mouse) for 3 weeks, followed by reperfusion for 2 h. After four weeks, the mice underwent Echo, followed by collecting blood and heart samples to analyze cardiac I/R injury. (B) Western blot was carried out to detect Fto protein levels in heart samples ($n = 3$). (C–E) Representative Echo images for mice in each group and cardiac function indices EF (%) and FS (%) ($n = 6$). (F,G) Serum CK-MB and TnT levels were analyzed by ELISA ($n = 6$). (H,I) Representative images and a quantitative histogram of Masson's staining on heart sections ($n = 6$). Scale bar: 500 μ m. (J) Total m6A levels in heart tissues were assessed with an anti-m6A antibody and colorimetric quantification ($n = 3$). (K) m6A-RIP-qPCR was conducted to analyze the enrichment m6A on *Anxa1* in heart tissues ($n = 3$). (L,M) Relative mRNA and protein levels of *Anxa1* in heart tissues were detected by RT-qPCR and western blot ($n = 3$). Data are shown as mean \pm SEM. Statistical analysis was performed using one-way ANOVA followed by Tukey's post hoc test in (B,D,E, and F–M); *** $p < 0.001$. Fto, fat mass and obesity-associated protein; I/R, ischemia-reperfusion; *Anxa1*, Annexin A1; MI, myocardial infarction; LAD, left anterior descending; adFto, adenovirus encoding Fto; adnull, a control vector for adFto; Echo, echocardiography; CK-MB, creatine kinase-myocardial; TnT, troponin T; ELISA, enzyme-linked immunosorbent assay; m6A, N6-methyladenosine; EF, ejection fraction; FS, fractional shortening; RIP, RNA immunoprecipitation; qPCR, quantitative polymerase chain reaction; SEM, standard error of the mean; ANOVA, analysis of variance; Gapdh, glyceraldehyde-3-phosphate dehydrogenase.

MB and cTnT in WT but not in *Anxa1*-KO ($p > 0.9999$), with a significant genotype \times treatment interaction (CK-MB: $F [2, 30] = 424.1$, $p < 0.001$; cTnT: $F [2, 30] = 14.79$,

$p < 0.001$) (Fig. 2E,F). In addition, heart sections of *Anxa1* KO mice presented a substantial elevation in collagen fibers post-MI, but Fto overexpression did not affect changes in

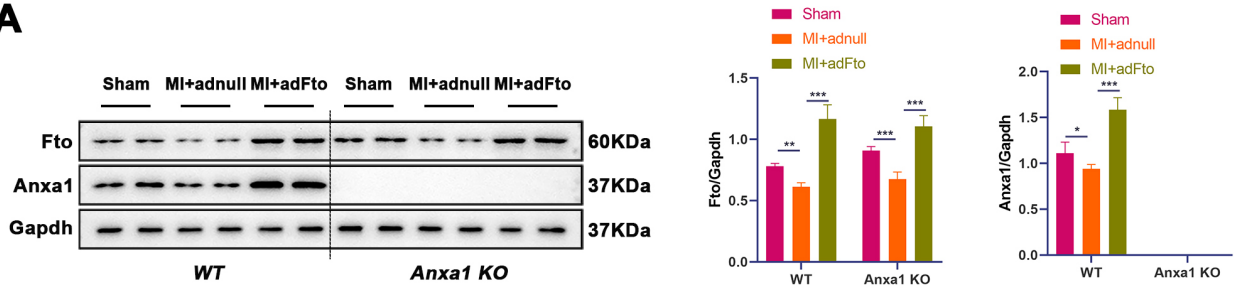
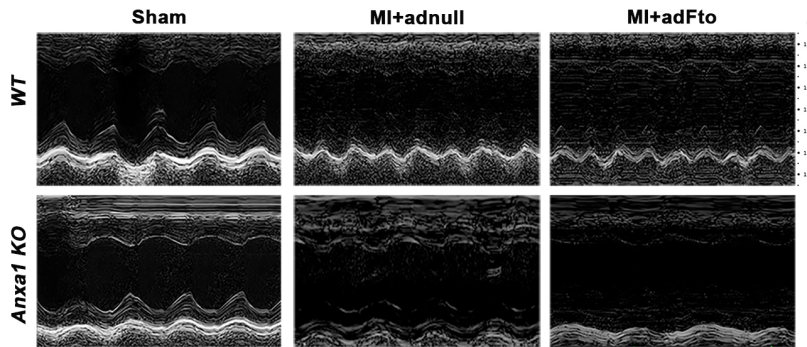
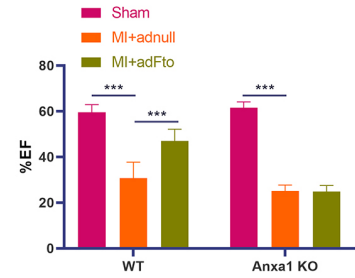
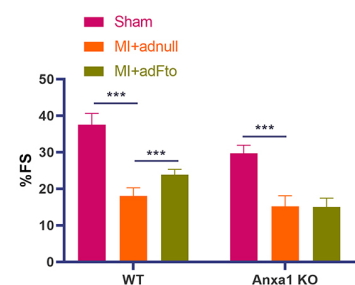
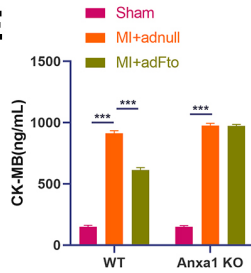
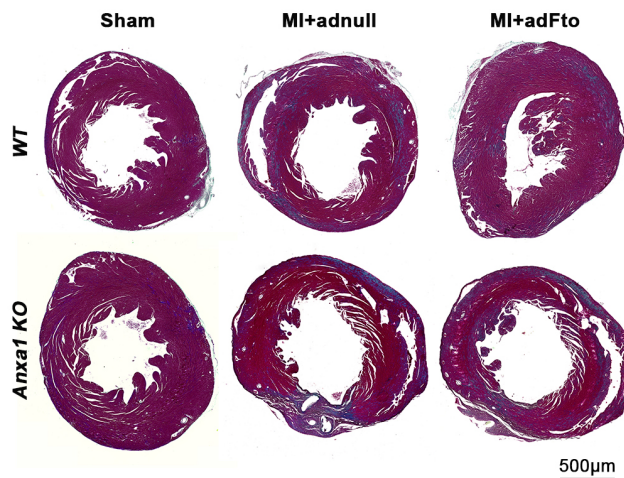
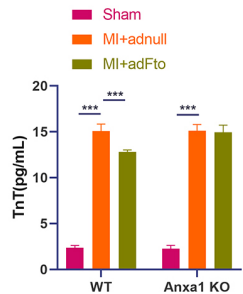
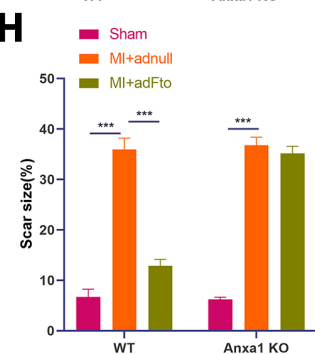
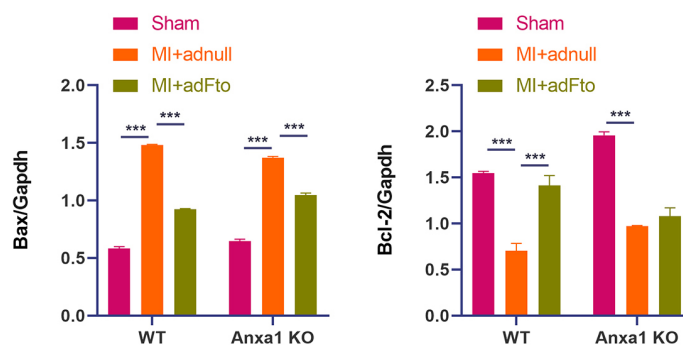
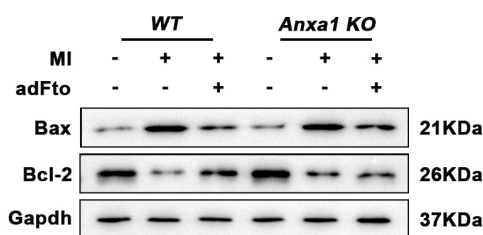
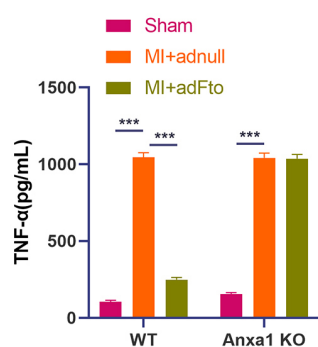
A**B****C****D****E****G****F****H**

Fig. 2. Fto mediates *Anxa1* expression against cardiac I/R injury. After intramyocardial injection of *adFto* or *adnull* (1×10^9 vg/mouse) for 3 weeks, both WT and *Anxa1* KO mice underwent sham or LAD occlusion for 30 min, followed by reperfusion for 2 h. (A) Protein levels of Fto and Anxa1 in heart samples from different groups were detected by western blot ($n = 3$). (B–D) Representative Echo images for mice in each group and histograms of cardiac function parameters EF (%) and FS (%) ($n = 6$). (E,F) Measurement of serum CK-MB and TnT levels was performed with ELISA ($n = 6$). (G,H) Representative images of Masson's staining with heart sections and a quantitative histogram for collagen fiber content ($n = 6$). Scale bar: 500 μm. Data are shown as mean \pm SEM. Statistical analysis was performed using two-way ANOVA followed by Tukey's post hoc test in (A, C–F, and H); * $p < 0.05$, ** $p < 0.01$, and *** $p < 0.001$. Fto, fat mass and obesity-associated protein; I/R, ischemia-reperfusion; *Anxa1*, Annexin A1; WT, wild type; KO, *Anxa1* knockout; LAD, left anterior descending; *adFto*, adenovirus encoding Fto; *adnull*, a control vector for *adFto*; Echo, echocardiography; CK-MB, creatine kinase-myocardial; TnT, troponin T; ELISA, enzyme-linked immunosorbent assay; EF, ejection fraction; FS, fractional shortening; SEM, standard error of the mean; ANOVA, analysis of variance.

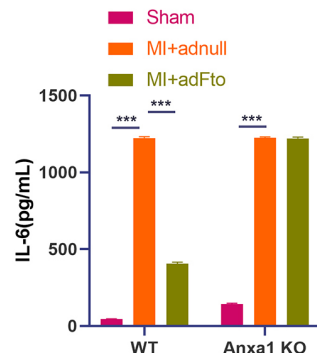
A



B



C



D

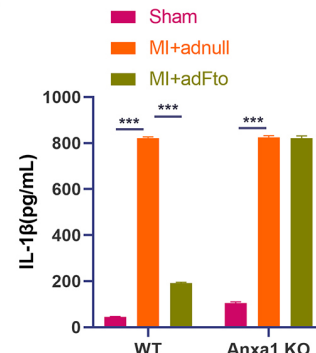


Fig. 3. Fto reduces cardiac apoptosis and inflammation via elevating *Anxa1* expression post-MI. (A) Protein levels of Bax and Bcl-2 in heart samples were detected by western blot (n = 3). (B–D) The levels of inflammatory cytokines (TNF-α, IL-6, and IL-1β) in heart samples were detected by ELISA (n = 6). Data are shown as mean ± SEM. Statistical analysis was performed using two-way ANOVA followed by Tukey's post hoc test in (A–D); ****p* < 0.001. Fto, fat mass and obesity-associated protein; *Anxa1*, Annexin A1; Bcl-2, B cell lymphoma-2; Bax, Bcl-2-associated X protein; TNF-α, tumor necrosis factor alpha; IL, interleukin; ELISA, enzyme-linked immunosorbent assay; EF, ejection fraction; FS, fractional shortening; SEM, standard error of the mean; ANOVA, analysis of variance.

cardiac collagen fibers following *Anxa1* knockout (36.76% vs. 35.15%, *p* = 0.2301) (interaction: *F* [2, 30] = 211.0, *p* < 0.001) (Fig. 2G,H). Together, these results suggested that Fto protects against cardiac I/R injury by increasing *Anxa1* expression.

3.3 Fto Attenuates Apoptosis and Inflammation in Cardiac Tissue Post-MI by Upregulating *Anxa1*

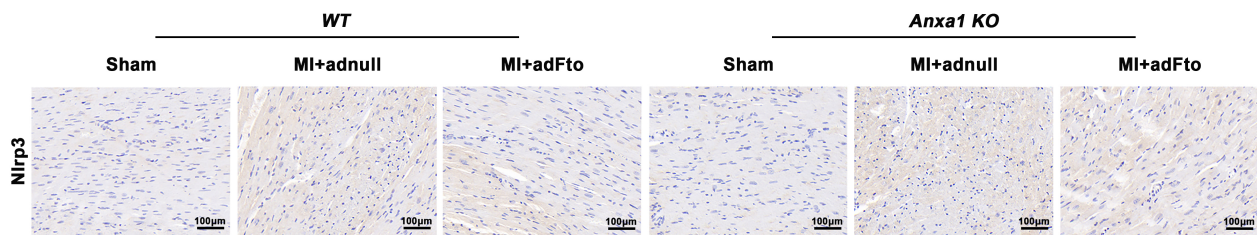
Given the pathological significance of apoptosis and inflammation in cardiac I/R injury after MI, we proceeded to analyze whether Fto exerts its effects on cardiac tissue apoptosis and inflammation via *Anxa1*. The results showed that cardiac samples from WT and *Anxa1* KO mice exhibited higher Bax protein levels and lower Bcl-2 protein levels after MI (*p* < 0.001). Fto overexpression partly reversed Bax protein levels in WT and *Anxa1* KO mice (*p* < 0.001), suggesting that Fto regulates Bax protein levels by mediating *Anxa1* and other genes. However, in *Anxa1* KO mice, the effect of adFto on the Bcl-2 restoration was absent (*p* = 0.2561) (interactions: *F* [2, 30] = 49.65, *p* < 0.001), suggesting that Fto regulates Bax protein levels primarily through mediating *Anxa1* expression (Fig. 3A). As for the

inflammatory response, cardiac samples of WT and *Anxa1* KO mice experiencing MI presented higher levels of TNF-α, IL-6, and IL-1β (*p* < 0.001), whereas Fto overexpression attenuated the levels of these inflammatory cytokines in WT mice (*p* < 0.001) but not in *Anxa1* KO mice (*p* = 0.8749 and *p* > 0.9999), yielding significant interactions (TNF-α: *F* [2, 30] = 1127, *p* < 0.001; IL-6: *F* [2, 30] = 11798, *p* < 0.001; IL-1β: *F* [2, 30] = 9273, *p* < 0.001), which suggested that Fto modulates inflammatory cytokines mainly through mediating *Anxa1* expression (Fig. 3B–D). Collectively, apoptotic and inflammatory readouts were attenuated by adFto in WT but not in *Anxa1* KO, in association with higher *Anxa1* expression, indicating that these benefits are linked to *Anxa1*.

3.4 Fto Inhibits Nlrp3 Inflammasome Activation and Pyroptosis After MI, in An *Anxa1*-dependent Manner

To verify the effect of the Fto/*Anxa1* axis on cardiac Nlrp3 activation and pyroptosis, we detected NLRP3 protein levels by IHC staining. As shown in Fig. 4A, Nlrp3 protein levels were higher in WT and *Anxa1* KO mouse-derived heart samples post-MI, yet Fto overexpression re-

A



B

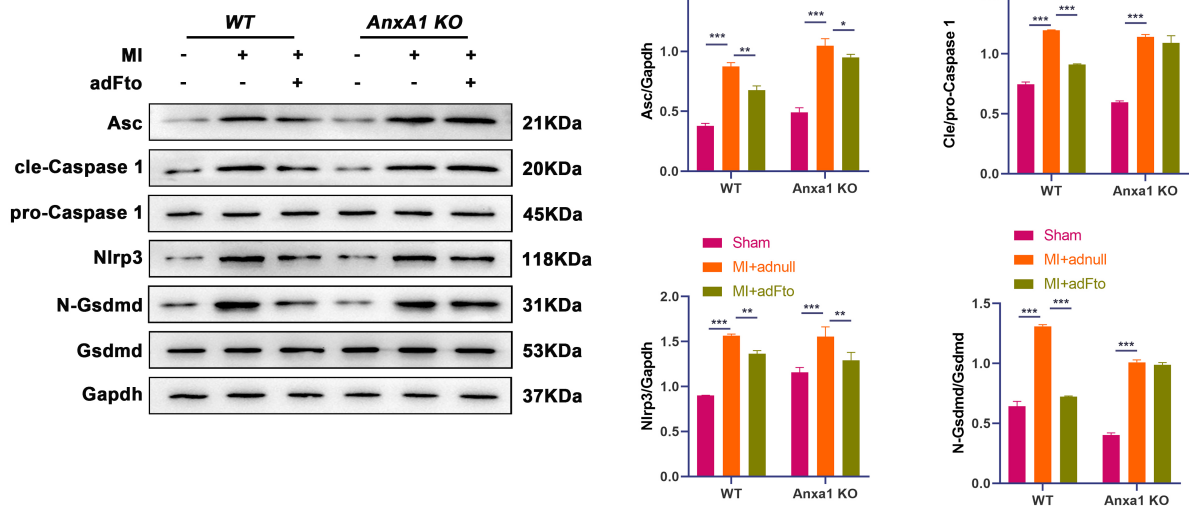


Fig. 4. Fto represses *Nlrp3*-mediated pyroptosis in the heart following MI through *Anxa1*. (A) IHC staining was conducted to detect *Nlrp3* protein levels in heart samples from different groups. Scale bar: 100 μ m. (B) Protein levels of ASC, cleaved caspase-1/pro caspase-1 ratio, *Nlrp3*, and N-Gsdmd/Gsdmd in heart samples were evaluated by western blot. Data are shown as mean \pm SEM. Statistical analysis was performed using two-way ANOVA followed by Tukey's post hoc test in (B); * p < 0.05, ** p < 0.01 and *** p < 0.001. Fto, fat mass and obesity-associated protein; *Nlrp3*, nucleotide-binding oligomerization domain-, leucine-rich repeat-, and pyrin domain- containing receptor 3; MI, myocardial infarction; *Anxa1*, Annexin A1; IHC, immunohistochemistry; ASC, apoptosis-associated speck-like protein, cle-Caspase 1, cleaved-Caspase 1; N-Gsdmd, gasdermin D-N-terminal domain; Gsdmd, gasdermin D; SEM, standard error of the mean; ANOVA, analysis of variance.

duced *Nlrp3* protein levels in WT mice but not in *Anxa1* KO mice. Additionally, higher protein levels of ASC, cleaved caspase-1/pro caspase-1 ratio, *Nlrp3*, and N-Gsdmd/Gsdmd were observed in heart samples of WT and *Anxa1* KO mice with MI (p < 0.001), whereas Fto up-regulation partially overturned the alteration of these proteins in the hearts of WT mice (p = 0.0064 and p < 0.001) but not *Anxa1* KO mice for cleaved caspase-1/pro caspase-1 ratio and N-Gsdmd/Gsdmd protein levels (p = 0.1346 and p = 0.8306) (ASC: F [2, 30] = 7.578, p = 0.0074; cleaved caspase-1/pro caspase-1 ratio: F [2, 30] = 56.30, p < 0.001; *Nlrp3*: F [2, 30] = 11.54, p = 0.0016; N-Gsdmd/Gsdmd: F [2, 30] = 292.9, p < 0.001;) (Fig. 4B). Altogether, these outcomes indicated that suppression of the *Nlrp3* axis and pyroptosis happens in conjunction with *Anxa1* upregulation downstream of Fto.

4. Discussion

The present study first demonstrated *in vivo* that *Anxa1* demethylation mediated by Fto-dependent demethylation of *Anxa1* is associated with attenuation of *Nlrp3* inflammasome activity and protection against myocardial I/R injury. These findings corroborate our previous *in vitro* observations and extend them to an intact physiological context, highlighting RNA methylation as a viable target for cardio-protection. From a translational standpoint, our findings align with broader cardioprotective and remodeling strategies; for instance, sodium glucose cotransporter 2 inhibitors have been linked to progenitor-cell modulation and favorable remodeling, offering convergent avenues to augment myocardial repair [22].

Currently, LAD ligation is an established method for establishing animal models of acute MI both at home and abroad. Among the various animal species used for modeling myocardial I/R injury, mice have become the most frequently employed due to their low cost and the availability of transgenic and knockout strains [23]. It has been demonstrated that irreversible myocardial damage occurs when ligation exceeds 30 min, while reperfusion for 1 to 24 h met the modelling criteria [24]. This study applied WT and *Anxa1* KO mice with a C57BL/6 background to construct cardiac I/R injury models, with ligation for 30 min and reperfusion for 2 h.

Fto, a key demethylase in the m6A system, plays a protective role in protecting against cardiac I/R injury. A prior study reported that Fto mRNA and protein levels were decreased significantly in ischemic aged hearts, indicating age-related differences in m6A regulation during cardiac I/R injury [25]. It was reported that down-regulation of Fto results in decreased Myc expression, enabling enhanced cardiomyocyte apoptosis and oxidative stress in hypoxia/reoxygenation (H/R)-induced cell models [26]. Ke *et al.* [27] demonstrated that Fto overexpression attenuates H/R-induced cardiomyocyte injury by suppressing cardiomyocyte apoptosis and inflammatory responses via removing the methylation modification of Yap1 mRNA. Consistent with previous studies [13,27], our findings also demonstrated that Fto ameliorated cardiac I/R injury, as evidenced by elevated left ventricular FS and EF values, reduced serum TnT and CK-MB levels, and improved cardiac fibrosis following Fto overexpression. These findings emphasize the crucial role of Fto in protecting against cardiac injury.

Anxa1 exhibits cardioprotective effects in cardiac injury. Singh *et al.* [28] suggested that *Anxa1* KO mice exhibit higher blood pressure than normal mice regardless of age, accompanied by cardiac dysfunction and cardiac hypertrophy, emphasizing the key role of *Anxa1* in regulating blood pressure, cardiovascular function and cardiac aging. Qi *et al.* [29] discovered that the activation of the *Anxa1*/G-protein coupled receptor formyl peptide receptor 2 axis can restrain neutrophil extracellular traps, thereby alleviating MI in rat models. F-box-only protein 32 exacerbates cardiac injury via mediating Anxa1 ubiquitination and repressing the phosphoinositide 3-kinase signaling [30]. Anxa1 small peptide prevents cardiomyocyte injury evoked by lipopolysaccharide via inhibition of ferroptosis-induced cell death, relying on sirtuin 3-dependent p53 deacetylation [31]. Here, we observed that exogenous expression of Fto weakened the increase in m6A levels in MI mouse-derived heart tissues, along with a significant elevation in *Anxa1* mRNA and protein levels, implying that Fto may improve cardiac I/R injury by mediating *Anxa1* expression in mouse models. As in WT mice, *Anxa1* KO mice subjected to MI possessed a marked decrease in EF and FS values, a sharp rise in serum CK-MB and cTnT levels, and an obvious el-

evation in collagen fibers, whereas Fto overexpression improved these parameters in WT mice but was ineffective in *Anxa1*-knockout mice, manifesting that Fto may protect against cardiac I/R injury post-MI by increasing *Anxa1* expression.

Mechanistically, myocardial I/R injury is characterized by a complex interplay of cardiomyocyte apoptosis, inflammatory cascade responses, and Nlrp3 inflammasome activation [32]. Cardiomyocyte apoptosis arises due to hypoxia, metabolic disturbances, and oxidative stress during myocardial I/R injury [33]. The release of cellular contents activates the immune system, triggering an inflammatory cascade that releases pro-inflammatory cytokines (such as IL-1 β and TNF- α), thus exacerbating myocardial damage [34]. The Nlrp3 inflammasome plays a pivotal role in this process and is activated by factors such as potassium efflux and mitochondrial dysfunction [35]. Once activated, it promotes caspase-1 maturation and activity, driving the release of IL-1 β and IL-18, which intensify pyroptosis and inflammation [36]. It is noteworthy that *Anxa1* modulates Nlrp3 inflammasome initiation and activation via an Fpr2 receptor-independent pathway [37]. In this study, we discovered that both WT and *Anxa1* KO mice exhibited elevated Bax protein and reduced Bcl-2 protein levels in cardiac tissues following MI, alongside increased levels of pro-inflammatory cytokines (TNF- α , IL-6, and IL-1 β) and pyroptosis-related proteins (ASC, cleaved caspase-1/pro caspase-1 ratio, Nlrp3, N-Gsdmd/Gsdmd). Fto overexpression partially reversed these alterations in WT mice but had minimal effects in *Anxa1* KO mice, with the exception of a modest reduction in Bax. Collectively, these findings indicated that Fto improves post-I/R outcomes and that *Anxa1* is an important mediator of this protection. At the transcript level, m6A-RIP-qPCR indicated reduced m6A enrichment on *Anxa1* with Fto overexpression, consistent with the dynamic nature of m6A regulation under stress. The protective phenotype is accompanied by lower Nlrp3-inflammasome activity together with attenuation of apoptosis and cytokine-driven inflammation. At the same time, *Anxa1* also participates in regulatory programs beyond Nlrp3, including control of apoptotic signaling, modulation of cytokine expression, and regulation of immune-cell recruitment and polarization in injured myocardium. We therefore regard the *Anxa1*-Nlrp3 axis as a major contributor rather than an exclusive mechanism. Future work using extended reperfusion windows, rescue designs, and pathway-specific perturbations will delineate the relative contributions of Nlrp3 and other *Anxa1*-linked pathways.

Several limitations should be acknowledged. First, the experiments were performed in young and healthy mice, which do not fully capture the molecular complexity and comorbid heterogeneity present in clinical MI, where conditions such as diabetes and hypertension are prevalent. Second, the study used a fixed ischemia duration, a prespecified acute 2-h reperfusion window, and a single adFto dose; ac-

cordingly, it does not establish temporal dynamics or dose–response relationships. Third, the specific m6A site of Fto-mediated *Anxa1* demethylation has not been clarified. Future studies will extend the reperfusion window (e.g., 24–72 h and 7–28 d) and perform dose-ranging to delineate the time course and exposure–response characteristics of the Fto–*Anxa1* axis and its relation to *Nlrp3* signaling, and identify the key m6A modification sites on *Anxa1* mRNA and evaluate the robustness of the Fto/*Anxa1* regulatory axis in db/db mice or aging models to enhance translational relevance.

5. Conclusions

Fto-mediated demethylation of *Anxa1* alleviates myocardial I/R injury with *Nlrp3* inflammasome suppression. Taken together, these *in vivo* data position the Fto–*Anxa1* axis as a major mechanistic contributor to protection against I/R and a promising target for future intervention.

Availability of Data and Materials

The datasets used and analyzed during the current study are available from the corresponding author on reasonable request.

Author Contributions

CJH, HJY and HLH designed experiments. HJY, LJX and HZ carried out experiments, analyzed experimental results. CJH and HJY wrote the manuscript. HLH revised the manuscript. All authors contributed to editorial changes in the manuscript. All authors read and approved the final manuscript. All authors have participated sufficiently in the work and agreed to be accountable for all aspects of the work.

Ethics Approval and Consent to Participate

All experimental procedures involving animals were undertaken in accordance with the National Institutes of Health guidelines and received approval from the Animal Care and Use Committee of Jiaying University Medical College (Approval No. JUMC2021-095).

Acknowledgment

Not applicable.

Funding

This work was supported by Jiaying Science and Technology Program (2023AY40029); Zhejiang Provincial Natural Science Foundation of China under Grant No. LQ23H020001; National Natural Science Foundation of China (No. 82300363); Zhejiang Province Clinical Key Specialty Construction Project (2024-ZJZK-001) and Jiaying Clinical Key Specialty Construction Project (2023-JXZK-001).

Conflict of Interest

The authors declare no conflict of interest.

Supplementary Material

Supplementary material associated with this article can be found, in the online version, at <https://doi.org/10.31083/FBL42765>.

References

- [1] Carberry J, Marquis-Gravel G, O'Meara E, Docherty KF. Where Are We With Treatment and Prevention of Heart Failure in Patients Post-Myocardial Infarction? *JACC. Heart Failure*. 2024; 12: 1157–1165. <https://doi.org/10.1016/j.jchf.2024.04.025>.
- [2] Ndrepepa G. Improving myocardial injury, infarct size, and myocardial salvage in the era of primary PCI for STEMI. *Coronary Artery Disease*. 2015; 26: 341–355. <https://doi.org/10.1097/MCA.0000000000000220>.
- [3] Welt FGP, Batchelor W, Spears JR, Penna C, Pagliaro P, Ibanez B, *et al*. Reperfusion Injury in Patients With Acute Myocardial Infarction: JACC Scientific Statement. *Journal of the American College of Cardiology*. 2024; 83: 2196–2213. <https://doi.org/10.1016/j.jacc.2024.02.056>.
- [4] Zhang S, Yan F, Luan F, Chai Y, Li N, Wang YW, *et al*. The pathological mechanisms and potential therapeutic drugs for myocardial ischemia reperfusion injury. *Phytomedicine: International Journal of Phytotherapy and Phytopharmacology*. 2024; 129: 155649. <https://doi.org/10.1016/j.phymed.2024.155649>.
- [5] Benak D, Kolar F, Hlavackova M. Epitranscriptomic Regulations in the Heart. *Physiological Research*. 2024; 73: S185–S198. <https://doi.org/10.33549/physiolres.935265>.
- [6] Zaccara S, Ries RJ, Jaffrey SR. Reading, writing and erasing mRNA methylation. *Nature Reviews. Molecular Cell Biology*. 2019; 20: 608–624. <https://doi.org/10.1038/s41580-019-0168-5>.
- [7] Zhou J, Wan J, Gao X, Zhang X, Jaffrey SR, Qian SB. Dynamic m(6)A mRNA methylation directs translational control of heat shock response. *Nature*. 2015; 526: 591–594. <https://doi.org/10.1038/nature15377>.
- [8] Engel M, Eggert C, Kaplick PM, Eder M, Röh S, Tietze L, *et al*. The Role of m⁶A/m-RNA Methylation in Stress Response Regulation. *Neuron*. 2018; 99: 389–403.e9. <https://doi.org/10.1016/j.neuron.2018.07.009>.
- [9] Xu ZY, Jing X, Xiong XD. Emerging Role and Mechanism of the *FTO* Gene in Cardiovascular Diseases. *Biomolecules*. 2023; 13: 850. <https://doi.org/10.3390/biom13050850>.
- [10] Yang Y, Ren J, Zhang J, Shi H, Wang J, Yan Y. FTO ameliorates doxorubicin-induced cardiotoxicity by inhibiting ferroptosis via P53-P21/Nrf2 activation in a HuR-dependent m6A manner. *Redox Biology*. 2024; 70: 103067. <https://doi.org/10.1016/j.redox.2024.103067>.
- [11] Sun F, An C, Liu C, Hu Y, Su Y, Guo Z, *et al*. FTO represses NLRP3-mediated pyroptosis and alleviates myocardial ischemia-reperfusion injury via inhibiting CBL-mediated ubiquitination and degradation of β -catenin. *FASEB Journal: Official Publication of the Federation of American Societies for Experimental Biology*. 2023; 37: e22964. <https://doi.org/10.1096/fj.202201793RR>.
- [12] Chang X, Zhou S, Liu J, Wang Y, Guan X, Wu Q, *et al*. Zishen Tongyang Huoxue decoction (TYHX) alleviates sinoatrial node cell ischemia/reperfusion injury by directing mitochondrial quality control via the VDAC1- β -tubulin signaling axis. *Journal of Ethnopharmacology*. 2024; 320: 117371. <https://doi.org/10.1016/j.jep.2023.117371>.

- [13] Jiang Q, Chen X, Gong K, Xu Z, Chen L, Zhang F. M6a demethylase FTO regulates the oxidative stress, mitochondrial biogenesis of cardiomyocytes and PGC-1 α stability in myocardial ischemia-reperfusion injury. *Redox Report: Communications in Free Radical Research*. 2025; 30: 2454892. <https://doi.org/10.1080/13510002.2025.2454892>.
- [14] Kelly L, McGrath S, Rodgers L, McCall K, Tulunay Virlean A, Dempsey F, *et al.* Annexin-A1: The culprit or the solution? *Immunology*. 2022; 166: 2–16. <https://doi.org/10.1111/imm.13455>.
- [15] D'Amico M, Di Filippo C, La M, Solito E, McLean PG, Flower RJ, *et al.* Lipocortin 1 reduces myocardial ischemia-reperfusion injury by affecting local leukocyte recruitment. *FASEB Journal: Official Publication of the Federation of American Societies for Experimental Biology*. 2000; 14: 1867–1869. <https://doi.org/10.1096/fj.99-0602je>.
- [16] La M, D'Amico M, Bandiera S, Di Filippo C, Oliani SM, Gavins FN, *et al.* Annexin 1 peptides protect against experimental myocardial ischemia-reperfusion: analysis of their mechanism of action. *FASEB Journal: Official Publication of the Federation of American Societies for Experimental Biology*. 2001; 15: 2247–2256. <https://doi.org/10.1096/fj.01-0196com>.
- [17] Qin C, Buxton KD, Pepe S, Cao AH, Venardos K, Love JE, *et al.* Reperfusion-induced myocardial dysfunction is prevented by endogenous annexin-A1 and its N-terminal-derived peptide Ac-ANX-A1(2-26). *British Journal of Pharmacology*. 2013; 168: 238–252. <https://doi.org/10.1111/j.1476-5381.2012.02176.x>.
- [18] Adel FW, Rikhi A, Wan SH, Iyer SR, Chakraborty H, McNulty S, *et al.* Annexin A1 is a Potential Novel Biomarker of Congestion in Acute Heart Failure. *Journal of Cardiac Failure*. 2020; 26: 727–732. <https://doi.org/10.1016/j.cardfail.2020.05.012>.
- [19] He C, Fan H, Zhu C, Huang Y. The up-regulation of ANXA1 by FTO-dependent demethylation alleviates NLRP3-mediated pyroptosis and inflammation in myocardial ischemia–reperfusion injury. *Molecular & Cellular Toxicology*. 2025; 1–12. <https://doi.org/10.1007/s13273-025-00513-6>.
- [20] Deng F, Zhang LQ, Wu H, Chen Y, Yu WQ, Han RH, *et al.* Propionate alleviates myocardial ischemia-reperfusion injury aggravated by Angiotensin II dependent on caveolin-1/ACE2 axis through GPR41. *International Journal of Biological Sciences*. 2022; 18: 858–872. <https://doi.org/10.7150/ijbs.67724>.
- [21] Livak KJ, Schmittgen TD. Analysis of relative gene expression data using real-time quantitative PCR and the 2(-Delta Delta C(T)) Method. *Methods (San Diego, Calif.)*. 2001; 25: 402–408. <https://doi.org/10.1006/meth.2001.1262>.
- [22] Stougiannou TM, Christodoulou KC, Koufakis T, Mitropoulos F, Mikroulis D, Mazer CD, *et al.* Progenitor Cell Function and Cardiovascular Remodelling Induced by SGLT2 Inhibitors. *Frontiers in Bioscience (Landmark Edition)*. 2024; 29: 145. <https://doi.org/10.31083/j.fbl2904145>.
- [23] Borst O, Ochmann C, Schönberger T, Jacoby C, Stellos K, Seizer P, *et al.* Methods employed for induction and analysis of experimental myocardial infarction in mice. *Cellular Physiology and Biochemistry: International Journal of Experimental Cellular Physiology, Biochemistry, and Pharmacology*. 2011; 28: 1–12. <https://doi.org/10.1159/000331708>.
- [24] De Villiers C, Riley PR. Mouse models of myocardial infarction: comparing permanent ligation and ischaemia-reperfusion. *Disease Models & Mechanisms*. 2020; 13: dmm046565. <https://doi.org/10.1242/dmm.046565>.
- [25] Su X, Shen Y, Jin Y, Kim IM, Weintraub NL, Tang Y. Aging-Associated Differences in Epitranscriptomic m6A Regulation in Response to Acute Cardiac Ischemia/Reperfusion Injury in Female Mice. *Frontiers in Pharmacology*. 2021; 12: 654316. <https://doi.org/10.3389/fphar.2021.654316>.
- [26] Wen C, Lan M, Tan X, Wang X, Zheng Z, Lv M, *et al.* GSK3 β Exacerbates Myocardial Ischemia/Reperfusion Injury by Inhibiting Myc. *Oxidative Medicine and Cellular Longevity*. 2022; 2022: 2588891. <https://doi.org/10.1155/2022/2588891>.
- [27] Ke WL, Huang ZW, Peng CL, Ke YP. m⁶A demethylase FTO regulates the apoptosis and inflammation of cardiomyocytes via YAP1 in ischemia-reperfusion injury. *Bioengineered*. 2022; 13: 5443–5452. <https://doi.org/10.1080/21655979.2022.2030572>.
- [28] Singh J, Jackson KL, Tang FS, Fu T, Nowell C, Salimova E, *et al.* The pro-resolving mediator, annexin A1 regulates blood pressure, and age-associated changes in cardiovascular function and remodeling. *FASEB Journal: Official Publication of the Federation of American Societies for Experimental Biology*. 2024; 38: e23457. <https://doi.org/10.1096/fj.202301802R>.
- [29] Qi M, Huang H, Li Z, Quan J, Wang J, Huang F, *et al.* Qingxin Jieyu Granule alleviates myocardial infarction through inhibiting neutrophil extracellular traps via activating ANXA1/FPR2 axis. *Phytomedicine: International Journal of Phytotherapy and Phytopharmacology*. 2024; 135: 156147. <https://doi.org/10.1016/j.phymed.2024.156147>.
- [30] Chen D, Liang X, Zhang L, Zhang J, Gao L, Yan D, *et al.* E3 Ubiquitin Ligase FBXO32 Promotes LPS-Induced Cardiac Injury by Regulating ANXA1/PI3K/AKT Signaling. *Inflammation*. 2025. <https://doi.org/10.1007/s10753-025-02273-w>. (online ahead of print)
- [31] Qin S, Ren Y, Feng B, Wang X, Liu J, Zheng J, *et al.* ANXA1sp Protects against Sepsis-Induced Myocardial Injury by Inhibiting Ferroptosis-Induced Cardiomyocyte Death via SIRT3-Mediated p53 Deacetylation. *Mediators of Inflammation*. 2023; 2023: 6638929. <https://doi.org/10.1155/2023/6638929>.
- [32] Francisco J, Del Re DP. Inflammation in Myocardial Ischemia/Reperfusion Injury: Underlying Mechanisms and Therapeutic Potential. *Antioxidants (Basel, Switzerland)*. 2023; 12: 1944. <https://doi.org/10.3390/antiox12111944>.
- [33] Xiang Q, Yi X, Zhu XH, Wei X, Jiang DS. Regulated cell death in myocardial ischemia-reperfusion injury. *Trends in Endocrinology and Metabolism: TEM*. 2024; 35: 219–234. <https://doi.org/10.1016/j.tem.2023.10.010>.
- [34] Algoet M, Janssens S, Himmelreich U, Gsell W, Pusovnik M, Van den Eynde J, *et al.* Myocardial ischemia-reperfusion injury and the influence of inflammation. *Trends in Cardiovascular Medicine*. 2023; 33: 357–366. <https://doi.org/10.1016/j.tcm.2022.02.005>.
- [35] Chen L, Mao LS, Xue JY, Jian YH, Deng ZW, Mazhar M, *et al.* Myocardial ischemia-reperfusion injury: The balance mechanism between mitophagy and NLRP3 inflammasome. *Life Sciences*. 2024; 355: 122998. <https://doi.org/10.1016/j.lfs.2024.122998>.
- [36] Shen S, Wang Z, Sun H, Ma L. Role of NLRP3 Inflammasome in Myocardial Ischemia-Reperfusion Injury and Ventricular Remodeling. *Medical Science Monitor: International Medical Journal of Experimental and Clinical Research*. 2022; 28: e934255. <https://doi.org/10.12659/MSM.934255>.
- [37] Galvão I, de Carvalho RVH, Vago JP, Silva ALN, Carvalho TG, Antunes MM, *et al.* The role of annexin A1 in the modulation of the NLRP3 inflammasome. *Immunology*. 2020; 160: 78–89. <https://doi.org/10.1111/imm.13184>.